

Article

Secondary Metabolites with α -Glucosidase Inhibitory Activity from the Mangrove Fungus *Mycosphaerella* sp. SYSU-DZG01

Pei Qiu ¹, Zhaoming Liu ^{1,2}, Yan Chen ¹, Runlin Cai ¹ , Guangying Chen ^{3,*} and Zhigang She ^{1,4,*} ¹ School of Chemistry, Sun Yat-Sen University, Guangzhou 510275, China² State Key Laboratory of Applied Microbiology Southern China, Guangdong Institute of Microbiology, Guangdong Academy of Sciences, Guangzhou 510070, China³ Key Laboratory of Tropical Medicinal Plant Chemistry of Ministry of Education, Hainan Normal University, Haikou 571158, China⁴ South China Sea Bio-Resource Exploitation and Utilization Collaborative Innovation Center, Guangzhou 510006, China

* Correspondence: chgying123@163.com (G.C.); ceshzhg@mail.sysu.edu.cn (Z.S.); Tel.: +86-20-8411-3356 (Z.S.)

Received: 29 July 2019; Accepted: 18 August 2019; Published: 20 August 2019



Abstract: Four new metabolites, asperchalsine I (**1**), dibefurin B (**2**) and two epicoccine derivatives (**3** and **4**), together with seven known compounds (**5–11**) were isolated from a mangrove fungus *Mycosphaerella* sp. SYSU-DZG01. The structures of compounds **1–4** were established from extensive spectroscopic data and HRESIMS analysis. The absolute configuration of **1** was deduced by comparison of ECD data with that of a known structure. The stereostructures of **2–4** were further confirmed by single-crystal X-ray diffraction. Compounds **1**, **8** and **9** exhibited significant α -glucosidase inhibitory activity with IC₅₀ values of 17.1, 26.7 and 15.7 μ M, respectively. Compounds **1**, **4**, **6** and **8** showed antioxidant activity by scavenging DPPH \cdot with EC₅₀ values ranging from 16.3 to 85.8 μ M.

Keywords: secondary metabolites; *Mycosphaerella* sp.; asperchalsine; α -glucosidase

1. Introduction

Diabetes mellitus (DM), a chronic metabolic disorder disease, is caused by the lack of insulin secretion (type I diabetes mellitus) or insufficient insulin sensitivity (type II diabetes mellitus) [1,2], and the typical characteristic of the latter is post-prandial hyperglycemia. α -Glucosidase is a kind of membrane-bounded enzyme which is mainly found in intestinal epithelium cells and leads to the increase of blood glucose levels by hydrolyzing the glycosidic bonds of a polysaccharide [3–5]. As a result of that, α -Glucosidase inhibitors (AGIs), such as acarbose, miglitol and voglibose have become a widespread medical treatment in type II diabetes mellitus according to their glycemic control ability [6,7]. Nevertheless, existing AGIs often cause many side effects including abdominal pain, flatulence, diarrhea and other gastrointestinal disorders [8,9]. Hence, many natural medicine chemists were attracted to develop α -glucosidase inhibitors with lower toxicity and side effects for potential use. Some new α -glucosidase inhibitors have been researched like flavipesolides A–C [10], asperterretal E [11] and so on [12,13], and the discovery of better α -glucosidase inhibitors is still an urgent need.

Marine fungi are proved to be rich sources of structurally unique and bioactive secondary metabolites. *Mycosphaerella* sp., which contributes the largest genus of Ascomycota, is a common plant pathogen widely distributed in terrestrial plant and marine environment [14–16]. As part of our ongoing investigation on new secondary metabolites from marine fungi in the South

China Sea [17–21], a mangrove fungus, *Mycosphaerella* sp. SYSU-DZG01, collected from the fruit of the mangrove plant *Bruguiera*, Hainan Dongzhai Harbor Mangrove Reserve attracted our attention because the EtOAc extract of the solid fermentation medium exhibited significant α -glucosidase inhibitory activity. Chemical investigation of the bioactive extract (Figure 1) led to the discovery of four new metabolites, asperchalsine I (1), dibefurin B (2) and two epicoccine derivatives, (*R*)-9-((*R*)-10-hydroxyethyl)-7,9-dihydroisobenzofuran-1-ol (3), 2-methoxycarbonyl-4,5,6-trihydroxy-3-methyl-benzaldehyde (4), together with seven known compounds, epicoccone B (5) [22], 1,3-dihydro-5-methoxy-7-methylisobenzofuran (6) [23], paeciloside A (7) [24], epicoccolide B (8) [25], asperchalsine A (9) [26], aspochalasin I (10) [27] and epicolactone (11) [28]. Their structures were established by extensive spectroscopic data and single-crystal X-ray diffraction analysis. Asperchalsine I possesses a distinct T-shaped skeleton containing one epicoccine moiety and one cytochalasan moiety. In bioactivity assays, compounds 1, 8 and 9 exhibited α -glucosidase inhibitory activity and 1, 4, 6 and 8 showed antioxidant activity by scavenging DPPH \cdot . Herein, the isolation, structure elucidation, α -glucosidase inhibitory and antioxidant activities of these compounds are reported.

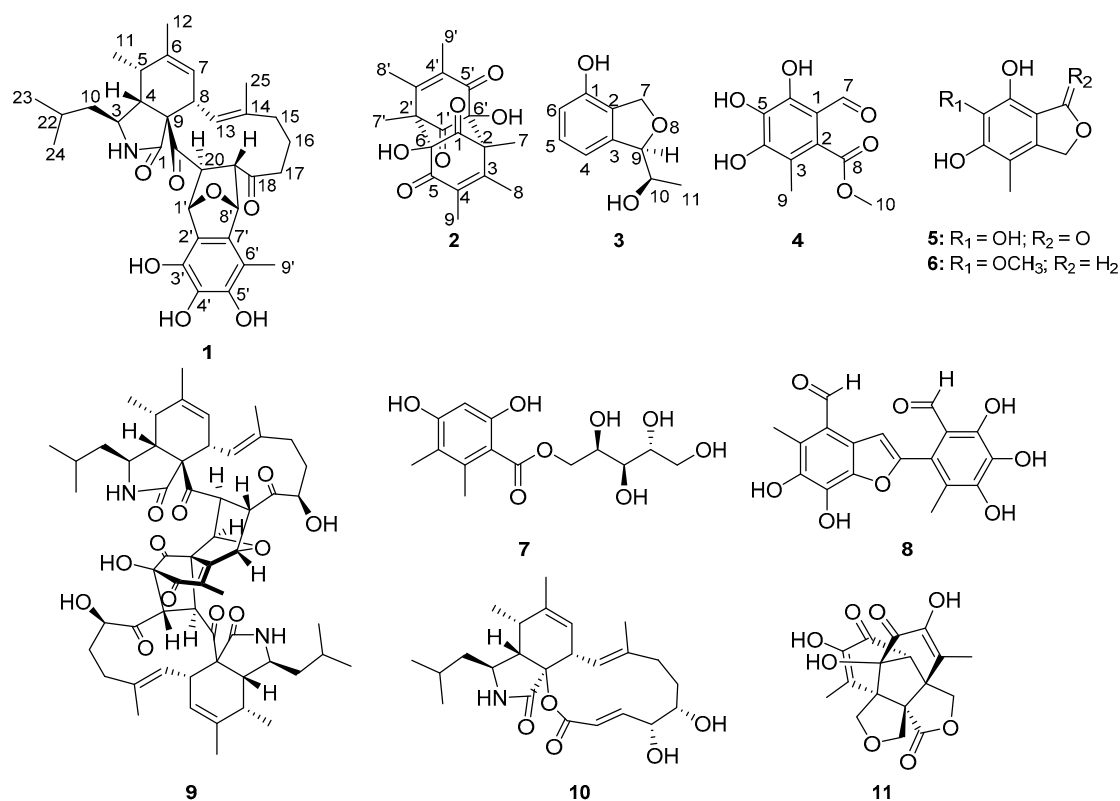


Figure 1. Chemical structures of 1–11.

2. Results

2.1. Structure Elucidation

Asperchalsine I (1), the molecular formula, $C_{33}H_{41}O_7N$, was determined on the basis of the HRESIMS ion at m/z 562.2798 ($[M - H]^-$ calcd. for $C_{33}H_{40}O_7N$: 562.2799). As shown in Table 1, the 1H NMR data indicated characteristic signals of two double-bond protons (δ_H 5.93 and 5.36), nine methine protons (δ_H 5.52, 5.06, 4.46, 3.76, 3.21, 3.05, 2.88, 2.54 and 1.62), four methylene protons (δ_H 2.09, 1.90, δ_H 2.01, 1.58, δ_H 1.35 and δ_H 1.21) and six methyl groups (δ_H 2.05, 1.78, 1.26, 1.17, 0.96 and 0.94). Subsequently, the ^{13}C NMR data showed the presence of 33 carbon signals, according to the DEPT and HSQC data, which were identified as three carbonyls (δ_C 211.6, 203.6 and 176.3), an aromatic ring (δ_C 141.3, 133.7, 132.6, 132.5, 123.7 and 111.9), two trisubstituted double bonds (δ_C 141.8, 137.4, 125.8 and

125.1), nine methines, four methylenes, six methyls and a quaternary carbon (δ_C 67.3). The ^1H - ^1H COSY (Figure 2) correlations of H₃-23/H-22/H₂-10/H-3/H-4/H-5/H₃-11, H-7/H-8/H-13, H₂-15/H₂-16/H₂-17 and H-19/H-20, together with the HMBC correlations from H-4 to C-1, C-9 and C-21, from H₃-12 to C-5, C-6 and C-7, from H-13 to C-25, from H₃-25 to C-15, from H₂-17 and H-19 to C-18, and from H-20 to C-21, suggested the presence of an cytochalasan moiety. Meanwhile, the epicoccine moiety was inferred by HMBC correlations from H-1' to C-3', from H-8' to C-2' and from H₃-9' to C-5', C-6' and C-7'. The key linking relation of the cytochalasan moiety and epicoccine moiety through C-19/C-8' and C-20/C-1' C-C bonds was suggested from the ^1H - ^1H COSY cross-peak of H-19/H-8' and the HMBC correlation from H-1' to C-20 and C-21. Moreover, the structure of **1** was further confirmed by a detailed comparison of the NMR data of **1** and asperchallasine B [26], which suggested that they shared the same skeleton. The upfield shifted of H₂-17 (δ_H 1.21) in **1** (δ_H 4.10 in asperchallasine B) and the disappearance of a methoxy group at C-4' (δ_H 3.70, δ_C 61.0), suggesting the replacements of methine at C-17 and a methoxy group at C-4' in asperchallasine B with a methylene and hydroxy group in **1**, respectively.

Table 1. ^1H (500 MHz) and ^{13}C (125 MHz) NMR data for **1** in CDCl₃.

| Position | 1 | |
|----------|-----------------------------|-----------------------|
| | δ_H , mult (J in Hz) | δ_C , Type |
| 1 | | 176.3, C |
| 2 | | |
| 3 | 3.21, m | 51.9, CH |
| 4 | 3.05, dd (3.9, 5.0) | 49.8, CH |
| 5 | 2.54, m, | 35.2, CH |
| 6 | | 141.8, C |
| 7 | 5.36, s | 125.1, CH |
| 8 | 2.88, d (11.1) | 43.3, CH |
| 9 | | 67.3, C |
| 10 | 1.35, t | 48.5, CH ₂ |
| 11 | 1.26, d (7.3) | 13.6, CH ₃ |
| 12 | 1.78, s | 20.1, CH ₃ |
| 13 | 5.93, d (11.0) | 125.8, CH |
| 14 | | 137.4, C |
| 15 | 2.09, s | 40.7, CH ₂ |
| | 1.90, d (4.3) | |
| 16 | 2.01, m | 22.5, CH ₂ |
| | 1.58, m | |
| 17 | 1.21, m | 35.1, CH ₂ |
| 18 | | 211.6, C |
| 19 | 3.76, t (5.3) | 56.9, CH |
| 20 | 4.46, d (5.8) | 57.3, CH |
| 21 | | 203.6, C |
| 22 | 1.62, m | 25.3, CH |
| 23 | 0.94, dd (1.2, 6.5) | 23.6, CH ₃ |
| 24 | 0.96, dd (1.2, 6.5) | 21.3, CH ₃ |
| 25 | 1.17, s | 14.2, CH ₃ |
| 1' | 5.06, s | 80.7, CH |
| 2' | | 123.7, C |
| 3' | | 132.5, C |
| 4' | | 133.7, C |
| 5' | | 141.3, C |
| 6' | | 111.9, C |
| 7' | | 132.6, C |
| 8' | 5.52, d (4.9) | 81.3, CH |
| 9' | 2.05, s | 11.9, CH ₃ |

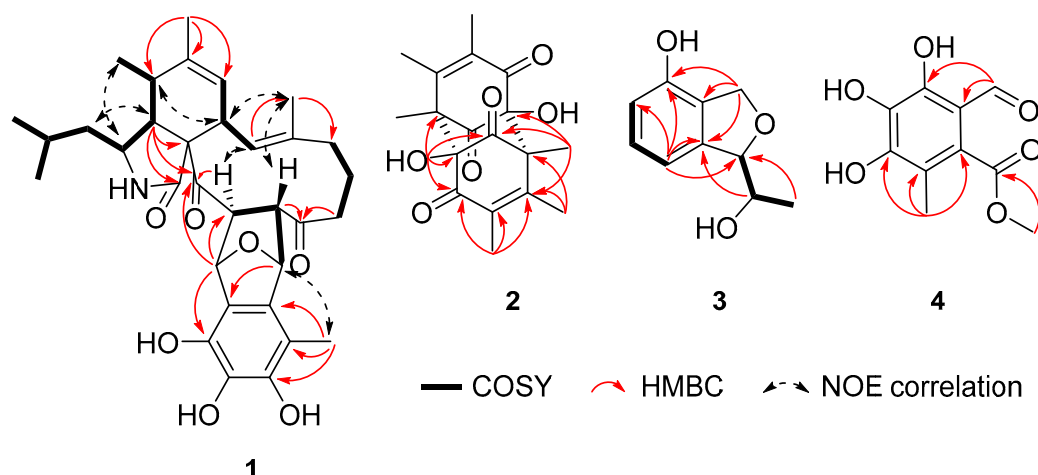


Figure 2. The key 2D NMR correlations of 1–4.

Detailed analysis of NOESY data determined the relative configuration of chiral carbons in compound **1**. The NOESY correlations of H-4/H₂-10, H-3/H₃-11, H-5/H-8/H₃-25, H-13/H-20 and H-19/H₃-25 suggested that these protons were cofacial. Neither ¹H-¹H coupling nor a ¹H-¹H COSY correlation was observed between the protons of H-20 (δ_{H} 4.46, d, J = 5.8 Hz) and H-1' (δ_{H} 5.06, s), which suggested that the dihedral angle of those protons was approximately 90° (Figure 3) [26]. The electron circular dichroism (ECD) spectrum (Figure S8) showed two positive Cotton effects (CE) at 228 nm and 306 nm, which were also consistent with those of aspercholasine B. Therefore, the absolute configuration of **1** was suggested to be 3*S*, 4*R*, 5*S*, 8*S*, 9*S*, 19*S*, 20*S*, 1'*S*, 8'*R*.

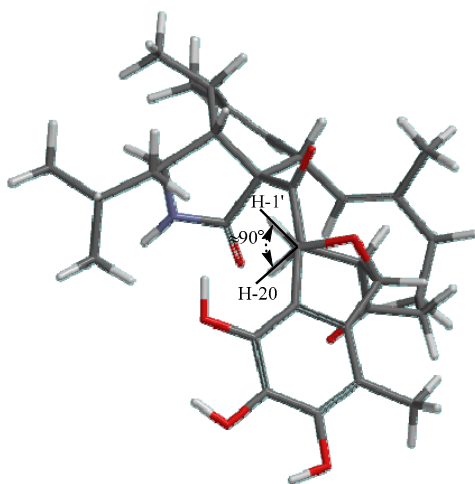


Figure 3. Molecular model of **1** (1'β, 8'β-oxygen bridge).

Dibefurin B (**2**), a colorless monocrystal, was assigned a molecular formula of C₁₈H₂₀O₆ by the HRESIMS ion at m/z 331.1187 ($[\text{M} - \text{H}]^-$ calcd. for C₁₈H₁₉O₆: 331.1187). For the monomer, the ¹H, ¹³C NMR (Table 2) and HSQC data of **2** revealed diagnostic signals for nine carbons, including two carbonyls (δ_{C} 200.6 and 192.6), two disubstituted olefin carbons (δ_{C} 157.6 and 131.4), an oxygen-bearing carbon [δ_{H} 6.67 (OH-6), δ_{C} 91.7 (C-6)], three methyls (δ_{C} 19.1, 12.2 and 12.1) and a quaternary carbon (δ_{C} 60.4). The HMBC correlations from H₃-7 to C-1, C-2, C-3 and C-6', from H₃-8 to C-2, C-3 and C-4, from H₃-9 to C-3, C-4 and C-5, revealed that Me-7, Me-8 and Me-9 were connected at C-2, C-3 and C-4, respectively. Similarly, the hydroxyl was attached to C-6, as evidenced by the HMBC correlations from OH-6 to C-1, C-2', C-5 and C-6. In view of the HRESIMS data and X-ray (Figure 4), it could confirm

that compound **2** was a symmetric dimer and the absolute configuration of **2** was assigned as 2*S*, 6*R*, 2'*R*, 6'*S*.

Table 2. ^1H (400 MHz) and ^{13}C (100 MHz) NMR data for **2** in $\text{DMSO-}d_6$.

| Position | 2 | |
|----------|--------------------------------------|----------------------------|
| | δ_{H} , mult (J in Hz) | δ_{C} , Type |
| 1 (1') | | 200.6, C |
| 2 (2') | | 60.4, C |
| 3 (3') | | 157.6, C |
| 4 (4') | | 131.4, C |
| 5 (5') | | 192.6, C |
| 6 (6') | | 91.7, C |
| 7 (7') | 1.21, s | 12.1, CH ₃ |
| 8 (8') | 2.02, s | 19.1, CH ₃ |
| 9 (9') | 1.73, s | 12.2, CH ₃ |

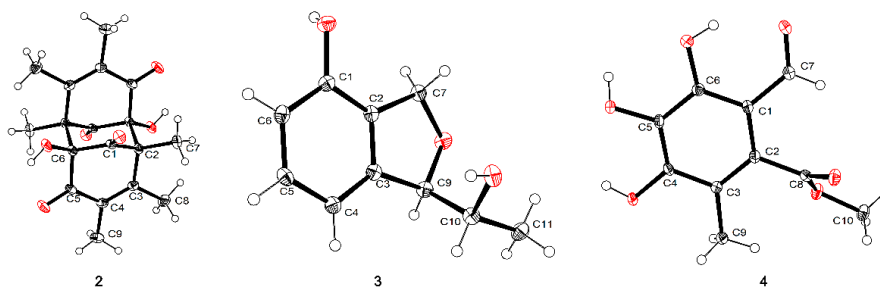


Figure 4. Single-crystal X-ray structures of **2–4**.

Compound **3** was purified as a colorless crystal whose molecular formula was deduced as $\text{C}_{10}\text{H}_{12}\text{O}_3$ based on HRESIMS data (179.0716 [$\text{M} - \text{H}$] $^-$, calcd. 179.0714). Analysis of the ^1H NMR spectrum of **3** (Table 3) displayed three aromatic proton resonances (δ_{H} 7.13, 6.82 and 6.69), an oxygenated methylene (δ_{H_a} 5.12, δ_{H_b} 5.02), two oxygenated methines (δ_{H} 5.06 and 3.97), and a methyl (δ_{H} 1.20). The ^{13}C spectrum revealed 10 signals, indicating an aromatic ring, a methylene, two methines and a methyl. In the ^1H - ^1H COSY spectrum, the ortho-trisubstitution on the aromatic ring was confirmed by the cross-peaks of H-4/H-5/H-6. Moreover, the ^1H - ^1H COSY spectrum showed correlations from H-10 to H-9 and H-11, and the chemical shift of C-10 (δ_{C} 70.6) showed the hydroxyl was attached to C-10. Subsequently, the HMBC correlations between H-6 and C-1/C-2 determined the linkage of 1-OH to C-1, and the correlations between H-7 and C-1/C-2/C-3, H-9 and C-2/C-3/C-10 established the presence of a phthalan ring. The same relative configuration of C-9 and C-10 was clearly deduced under the guidance of single-crystal X-ray (Figure 4). Hence, the absolute configuration of **3** was determined as 9*R*, 10*R*.

Compound **4** was deduced to have a molecular formula of $\text{C}_{10}\text{H}_{10}\text{O}_6$ from its HRESIMS spectrum with a deprotonated molecular ion at m/z 225.0407. The ^1H NMR (Table 3) in $\text{MeOH-}d_4$ showed three singlets at δ_{H} 9.71, 3.90 and 2.08, according to the ^{13}C NMR and HSQC data, which were attributed to an aldehyde group (δ_{C} 194.7), a methoxy group (δ_{C} 52.9) and a methyl (δ_{C} 12.4), respectively. In addition, resonances of a carbonyl and an aromatic ring were observed in the ^{13}C NMR data. In the HMBC spectrum, the correlations of H-9 to C-2, C-3 and C-4 supported the connection of Me-9 to C-3, the correlations of H-7 to C-1 and C-6 indicated the linkage of aldehyde group and C-1. Meanwhile, the carbonyl (δ_{C} 169.9, C-8) had the HMBC correlation from H-10 (δ_{H} 3.90), further indicated the presence of methyl ester. With the assistance of single-crystal X-ray (Figure 4), the structure of compound **4** was clearly confirmed.

Table 3. ^1H and ^{13}C NMR data for **3** and **4** in $\text{MeOH-}d_4$.

| Position | 3 ^a | | 4 ^b | |
|----------|--|----------------------------|--------------------------------------|----------------------------|
| | δ_{H} , mult (J in Hz) | δ_{C} , Type | δ_{H} , mult (J in Hz) | δ_{C} , Type |
| 1 | | 152.8, C | | 112.2, C |
| 2 | | 127.3, C | | 117.4, C |
| 3 | | 142.1, C | | 129.9, C |
| 4 | 6.82, d (7.4) | 114.3, CH | | 152.5, C |
| 5 | 7.13, t (7.7) | 129.9, CH | | 134.1, C |
| 6 | 6.69, d (7.9) | 115.0, CH | | 151.2, C |
| 7 | 5.12, dd (2.8, 11.8) 5.02, d (11.9) | 72.4, CH ₂ | 9.71, s | 194.7, CH |
| 8 | | | | 169.9, C |
| 9 | 5.06, d (3.3) | 89.4, CH | 2.08, s | 12.4, CH ₃ |
| 10 | 3.97, qd (3.9, 6.4) | 70.6, CH | 3.90, s | 52.9, CH ₃ |
| 11 | 1.20, d (6.4) | 18.6, CH ₃ | | |

^a ^1H and ^{13}C NMR recorded at 500 MHz and 125 MHz; ^b ^1H and ^{13}C NMR recorded at 400 MHz and 100 MHz.

2.2. Biological Evaluation

Compounds **1–11** were tested for their inhibitory effects against α -glucosidase, and antioxidant activity. As seen in Table 4, the results indicated that compounds **1**, **8** and **9** showed significant inhibitory effects against α -glucosidase with IC_{50} values of 17.1, 26.7 and 15.7 μM , respectively, which were better than the positive controls acarbose (610.2 μM) and 1-deoxynojirimycin (71.5 μM). Beyond that, all of the compounds were tested for their antioxidant activity based on DPPH \cdot (2, 2-diphenyl-1-picrylhydrazyl radical) scavenging. The results showed the antioxidant activity of **8** was 89% at the concentration of 100 μM and compound **8** possessed more potent capacity than positive control ascorbic acid in scavenging DPPH \cdot with an EC_{50} value of 16.3 μM . Compounds **1**, **4** and **6** also exhibited weak DPPH \cdot scavenging activity with respective EC_{50} values of 77.8, 85.8 and 59.1 μM .

Table 4. The α -glucosidase inhibitory and antioxidant activities of compounds **1–11**.

| Compounds | α -Glucosidase Inhibitory | | Antioxidant | |
|---------------------------------|------------------------------------|-----------------------------------|------------------------------------|--|
| | IC_{50} (μM) | % Inhibition (100 μM) | EC_{50} (μM) | |
| 1 | 17.1 | 56 | 77.8 | |
| 2 | >50 | <50 | - | |
| 3 | >50 | <50 | - | |
| 4 | >50 | 57 | 85.8 | |
| 5 | >50 | <50 | - | |
| 6 | >50 | 65 | 59.1 | |
| 7 | >50 | <50 | - | |
| 8 | 26.7 | 89 | 16.3 | |
| 9 | 15.7 | <50 | - | |
| 10 | - | - | - | |
| 11 | >50 | <50 | - | |
| Acarbose ^a | 610.2 | | | |
| 1-Deoxynojirimycin ^a | 71.5 | | | |
| Ascorbic acid ^a | | 92 | 22.4 | |

- means no test; ^a positive control.

3. Experimental Section

3.1. General Experimental Procedures

UV data were measured on a UV-Vis-NIR spectrophotometer (Perkin Elmer, Waltham, UK). IR spectrum data were recorded using a Bruker Vector spectrophotometer 22. Melting points

were tested on a Fisher-Johns hot-stage apparatus which were uncorrected. Optical rotations were recorded using an MCP300 (Anton Paar, Shanghai, China). HRESIMS data were conducted on an Ion Mobility-Q-TOF High-Resolution LC-MS (Synapt G2-Si, Waters). The ECD experiment data were measured with J-810 spectropolarimeter (JASCO, Tokyo, Japan). The NMR spectra were recorded on Bruker Avance spectrometer (Bruker, Beijing, China) (Compounds **1** and **3**: 500 MHz for ^1H and 125 MHz for ^{13}C , respectively; compounds **2** and **4**: 400 MHz for ^1H and 100 MHz for ^{13}C). Column chromatography (CC) was carried out on silica gel (200–300 mesh, Marine Chemical Factory, Qingdao, China) and sephadex LH-20 (Amersham Pharmacia, Piscataway, NJ, USA).

3.2. Fungal Materials

The fungus used in this research was isolated from the fruit of the marine mangrove plant *Bruguiera* collected in 2014 in Hainan Dongzhai Harbor Mangrove Reserve by using the standard protocol. The strain was identified as *Mycosphaerella* sp. (compared to no. KX067865.1) upon the analysis of ITS sequence data of the rDNA gene. The ITS sequence data obtained from the fungal strain has been submitted to GenBank with accession no. MN194208. A voucher strain was deposited in our laboratory.

3.3. Fermentation, Extraction and Isolation

The fungus *Mycosphaerella* sp. SYSU-DZG01 was grown on solid cultured medium in 100×1000 mL Erlenmeyer flasks at room temperature for 30 days under static conditions, each containing 80 g rice and 120 mL 0.3% saline. After incubation, the former was extracted with methanol twice and concentrated to yield 10.9 g of crude extract under reduced pressure. The crude extract was subjected to LC-HRESIMS analysis (Figure S29). Then, the residue was eluted by using gradient elution with petroleum ether/EtOAc from 9:1 to 0:10 (*v/v*) on silica gel CC to get ten fractions (Fr.1–Fr.10). Fr.2 (630 mg) was further eluted by silica gel CC using $\text{CH}_2\text{Cl}_2/\text{MeOH}$ (40:1) to obtain Fr.2.1–Fr.2.3. Fr.2.3 (301 mg) was purified by Sephadex LH-20 CC and eluted with MeOH to obtain compound **2** (3.5 mg), **6** (11.1 mg) and **10** (3.6 mg). Fr.4 (217 mg) was applied to silica gel CC by $\text{CH}_2\text{Cl}_2/\text{MeOH}$ (20:1) to obtain Fr.4.1–Fr.4.7. Fr.4.1 (8.1 mg) was further purified by Sephadex LH-20 CC using MeOH to obtain compound **1** (2.3 mg), **3** (2.2 mg), **8** (20.8 mg) and **9** (2.7 mg). Fr.5 (817 mg) was eluted (by $\text{CH}_2\text{Cl}_2/\text{MeOH}$, 25:3) to obtain Fr.5.1–Fr.5.5. Fr.5.1 (13.3 mg), Fr.5.2 (27.7 mg) and Fr.5.4 (10.9 mg) was purified by Sephadex LH-20 CC using $\text{CH}_2\text{Cl}_2/\text{MeOH}$ (1:1) to yield compound **4** (4.3 mg), **5** (2.0 mg), **7** (3.7 mg) and **11** (2.7 mg).

Asperchalsine I (**1**): White powder; $[\alpha]_{\text{D}}^{25} = +61.4$ (*c* 0.1, MeOH); UV (MeOH) λ_{max} ($\log \epsilon$): 206 (4.53) nm; IR (KBr) ν_{max} (cm^{-1}): 3369, 1691, 1440, 1384, 1201, 1120, 1053; HRESIMS m/z 562.2798 $[\text{M} - \text{H}]^-$ (calcd. for $\text{C}_{33}\text{H}_{40}\text{O}_7\text{N}$: 562.2799); ^1H and ^{13}C NMR data: see Table 1.

Dibefurin B(**2**): Colorless crystal; m.p. 67.8–69.2 °C; $[\alpha]_{\text{D}}^{25} = +0.3$ (*c* 0.1, MeOH); UV (MeOH) λ_{max} ($\log \epsilon$): 237 (3.98) nm; IR (KBr) ν_{max} (cm^{-1}): 3448, 1747, 1664, 1645, 1238, 1037; HRESIMS m/z 331.1187 $[\text{M} - \text{H}]^-$ (calcd. for $\text{C}_{18}\text{H}_{19}\text{O}_6$, 331.1187); ^1H and ^{13}C NMR data: see Table 2.

Compound **3**: Colorless crystal; m.p. 89.8–91.9 °C; $[\alpha]_{\text{D}}^{25} = -37.1$ (*c* 0.1, MeOH); UV (MeOH) λ_{max} ($\log \epsilon$) 204 (4.39), 269 (3.24) nm; IR (KBr) ν_{max} (cm^{-1}): 3261, 2887, 1601, 1471, 1297, 767, 706; HRESIMS m/z 179.0716 $[\text{M} - \text{H}]^-$ (calcd. for $\text{C}_{10}\text{H}_{12}\text{O}_3$, 179.0714); ^1H and ^{13}C NMR data: see Table 2.

Compound **4**: Colorless crystal; m.p. 95.9–97.8 °C; $[\alpha]_{\text{D}}^{25} = +3.4$ (*c* 0.1, MeOH); UV (MeOH) λ_{max} ($\log \epsilon$) 241 (3.66), 305 (3.56) nm; IR (KBr) ν_{max} (cm^{-1}): 3375, 2962, 1711, 1641, 1261, 1150, 933; HRESIMS m/z 225.0407 $[\text{M} - \text{H}]^-$ (calcd. for $\text{C}_{10}\text{H}_{10}\text{O}_6$, 225.0407); ^1H and ^{13}C NMR data: see Table 2.

3.4. X-Ray Crystallographic Data

Colorless crystals of compounds **2–4** were obtained from MeOH-CH₂Cl₂ at room temperature by slow volatilization, and examined on an Agilent Xcalibur Nova single crystal diffractometer with Cu K α radiation.

The crystallographic data for compound **2** has been deposited in the Cambridge Crystallographic Data Centre (CCDC number: 18022803)

Crystal data of **2**: C₁₈H₂₀O₆, *Mr* = 332.34, triclinic, *a* = 6.9740(4) Å, *b* = 7.9800(4) Å, *c* = 14.3659(6) Å, α = 101.148(4)°, β = 99.209(4)°, γ = 98.479(5)°, *V* = 761.05(7) Å³; space group *P*-1, *Z* = 2, *Dc* = 1.450 g/cm³, μ = 0.908 mm⁻¹ and *F*(000) = 352.0; Crystal dimensions: 0.40 × 0.30 × 0.02 mm³. Independent reflections: 4998 (*R*_{int} = 0.0269). The final *R*₁ was 0.0522, *wR*₂ = 0.1447 [*I* > 2 σ (*I*)]. The goodness of fit on *F*² was 1.048.

The crystallographic data for compound **3** has been deposited in the Cambridge Crystallographic Data Centre (CCDC number: 18121203)

Crystal data of **3**: C₁₀H₁₂O₃, *Mr* = 180.07, monoclinic, *a* = 4.7697(1) Å, *b* = 11.1895(3) Å, *c* = 9.1541(3) Å, α = 90°, β = 93.829(3)°, γ = 90°, *V* = 487.47(2) Å³; space group *P*21, flack 0.14(18), *Z* = 2, *Dc* = 1.350 g/cm³, μ = 0.872 mm⁻¹ and *F*(000) = 212.0; Crystal dimensions: 0.40 × 0.10 × 0.05 mm³. Independent reflections: 7438 (*R*_{int} = 0.0620). The final *R*₁ was 0.0445, *wR*₂ = 0.1258 [*I* > 2 σ (*I*)]. The goodness of fit on *F*² was 1.046.

The crystallographic data for compound **4** has been deposited in the Cambridge Crystallographic Data Centre (CCDC number: 18120705)

Crystal data of **4**: C₁₀H₁₀O₆, *Mr* = 226.04, orthorhombic, *a* = 15.9208(7) Å, *b* = 6.6849(3) Å, *c* = 18.5162(7) Å, α = 90°, β = 90°, γ = 90°, *V* = 1970.66(14) Å³; space group *Pbca*, *Z* = 8, *Dc* = 1.525 g/cm³, μ = 1.108 mm⁻¹ and *F*(000) = 944.0; Crystal dimensions: 0.25 × 0.03 × 0.03 mm³. Independent reflections: 3833 (*R*_{int} = 0.0496). The final *R*₁ was 0.0485, *wR*₂ = 0.1328 [*I* > 2 σ (*I*)]. The goodness of fit on *F*² was 1.050.

3.5. Biological Assays

3.5.1. Inhibitory Activity of α -Glucosidase

The α -glucosidase inhibitory activity was assayed according to the reported method [29]. The inhibitory activity of α -glucosidase was tested in the 96-well plated with 100 mM PBS (KH₂PO₄-K₂HPO₄, pH 7.0) buffer solution each. Compounds **1–11**, acarbose and 1-deoxynojirimycin (positive control) were dissolved in DMSO, the substrate (*p*-nitrophenyl glycoside, 5 mM) were dissolved in PBS buffer solution and enzyme solutions (2.0 units/mL) were prepared. The assay was conducted in a 100 μ L reaction system containing 20 μ L enzyme stock solution, 69 μ L PBS buffers and 1 μ L of DMSO or testing materials. After 10 min incubation at 37 °C, 10 μ L of the substrate was added and incubated for 20 min at 37 °C. The Absorbance which measured by a BIO-RAD (iMark) microplate reader at 405 nm was used to calculate the inhibitory activity according to the equation:

$$\eta (\%) = [(B - S)/B] \times 100\% \quad (1)$$

η (%) is the percentage of inhibition; B is the assay medium with DMSO; S is the assay medium with compound. The results of IC₅₀ values were calculated by the nonlinear regression analysis. Acarbose and 1-deoxynojirimycin were used as positive controls.

3.5.2. Antioxidant Activity

The DPPH \cdot scavenging was assayed according to the reported method [30]. The DPPH radical scavenging test was performed in 96-well microplates. Testing materials (compounds **1–11**) were added to 150 μ L (0.16 mmol/L) DPPH solution in MeOH at a range of 50 μ L solutions of different

concentrations (2, 25, 50 and 100 μM). After 30 min, absorbance at 517 nm was measured and the percentage of activity was calculated. Ascorbic acid was used as a positive control.

4. Conclusions

In summary, four new metabolites, including one new asperchalasine I (**1**), dibefurin B (**2**), two epicoccine derivatives (**3,4**) and seven known compounds were isolated from the fungus *Mycosphaerella* sp. SYSU-DZG01. The structures of **1–11** were established by spectroscopic data and the absolute configuration of compounds **1–3** was determined in this research. Compound **1** possesses a unique T-shaped skeleton. All of the compounds were tested for their biological activities. Compounds **1**, **8** and **9** exhibited inhibitory effects against α -glucosidase with IC_{50} values of 17.1, 26.7 and 15.7 μM , respectively while compounds **1**, **4**, **6** and **8** showed antioxidant activity by scavenging DPPH· with EC_{50} values of 77.8, 85.8, 59.1 and 16.3 μM . These results suggested that the asperchalasine I may be a potential candidate for α -glucosidase inhibitor.

Supplementary Materials: The following are available online at <http://www.mdpi.com/1660-3397/17/8/483/s1>, Figure S1: ^1H NMR spectrum of compound **1** (500 MHz, CDCl_3), Figure S2: ^{13}C NMR spectrum of compound **1** (125 MHz, CDCl_3), Figure S3: DEPT 135, DEPT 90 and ^{13}C NMR spectrum of compound **1** (125 MHz, CDCl_3), Figure S4: ^1H - ^1H COSY spectrum of compound **1** (CDCl_3), Figure S5: HSQC spectrum of compound **1** (CDCl_3), Figure S6: HMBC spectrum of compound **1** (CDCl_3), Figure S7: NOESY spectrum of compound **1** (CDCl_3), Figure S8: HRESIMS spectrum of compound **1**, Figure S9: Experiment ECD spectrum of **1**, Figure S10: ^1H NMR spectrum of compound **2** (400 MHz, $\text{DMSO-}d_6$), Figure S11: ^{13}C NMR spectrum of compound **2** (100 MHz, $\text{DMSO-}d_6$), Figure S12: ^1H - ^1H COSY spectrum of compound **2** ($\text{DMSO-}d_6$), Figure S13: HSQC spectrum of compound **2** ($\text{DMSO-}d_6$), Figure S14: HMBC spectrum of compound **2** ($\text{DMSO-}d_6$), Figure S15: HRESIMS spectrum of compound **2**, Figure S16: ^1H NMR spectrum of compound **3** (500 MHz, $\text{MeOH-}d_4$), Figure S17: ^{13}C NMR spectrum of compound **3** (125 MHz, $\text{MeOH-}d_4$), Figure S18: ^1H - ^1H COSY spectrum of compound **3** ($\text{MeOH-}d_4$), Figure S19: HSQC spectrum of compound **3** ($\text{MeOH-}d_4$), Figure S20: HMBC spectrum of compound **3** ($\text{MeOH-}d_4$), Figure S21: NOESY spectrum of compound **3** ($\text{MeOH-}d_4$), Figure S22: HRESIMS spectrum of compound **3**, Figure S23: ^1H NMR spectrum of compound **4** (400 MHz, $\text{MeOH-}d_4$), Figure S24: ^{13}C NMR spectrum of compound **4** (100 MHz, $\text{MeOH-}d_4$), Figure S25: ^1H - ^1H COSY spectrum of compound **4** ($\text{MeOH-}d_4$), Figure S26: HSQC spectrum of compound **4** ($\text{MeOH-}d_4$), Figure S27: HMBC spectrum of compound **4** ($\text{MeOH-}d_4$), Figure S28: HRESIMS spectrum of compound **4**. Figure S29: The LC-HRESIMS analysis profile of crude extract.

Author Contributions: P.Q. contributed to isolation, structure elucidation and wrote the paper; Z.L. contributed to the analysis of the NMR data and structure elucidation. Y.C. contributed to the analysis of the NMR data and biological tests. R.C. contributed to the spectral analysis. Z.S. and G.C. guided the whole experiment and revised the manuscript.

Funding: This research was funded by the Guangdong Special Fund for Marine Economic Development (GDME-2018C004), Guangdong MEPP Fund (GDOE-2019A21), the National Natural Science Foundation of China (2187713, 21472251), the Key Project of Natural Science Foundation of Guangdong Province (2016A040403091), the Special Promotion Program for Guangdong Provincial Ocean and Fishery Technology (A201701C06) and the open foundation of Key Laboratory of Tropical Medicinal Resource Chemistry of Ministry of Education (rdyw2018001).

Acknowledgments: We thank all the funding assistance mentioned above for their generous support and the Sun Yat-Sen University Instrumental Analysis and Research Center.

Conflicts of Interest: The authors declare no conflict of interest.

References

1. Wresdiyati, T.; Sa'Diah, S.; Winarto, A.; Febriyani, V. Alpha-Glucosidase Inhibition and Hypoglycemic Activities of Sweitenia mahagoni Seed Extract. *HAYATI J. Biosci.* **2015**, *22*, 73–78. [[CrossRef](#)]
2. Sekar, V.; Chakraborty, S.; Mani, S.; Sali, V.K.; Vasanthi, H.R. Mangiferin from Mangifera indica fruits reduces post-prandial glucose level by inhibiting α -glucosidase and α -amylase activity. *S. Afr. J. Bot.* **2019**, *120*, 129–134. [[CrossRef](#)]
3. Wang, H.; Du, Y.J.; Song, H.C. α -Glucosidase and α -amylase inhibitory activities of guava leaves. *Food Chem.* **2010**, *123*, 6–13. [[CrossRef](#)]

4. Tang, H.; Ma, F.; Zhao, D.; Xue, Z. Exploring the effect of salvianolic acid C on α -glucosidase: Inhibition kinetics, interaction mechanism and molecular modelling methods. *Process. Biochem.* **2019**, *78*, 178–188. [[CrossRef](#)]
5. Indrianingsih, A.W.; Tachibana, S. α -Glucosidase inhibitor produced by an endophytic fungus, *Xylariaceae* sp. QGS 01 from *Quercus gilva* Blume. *Food Sci. Hum. Wellness* **2017**, *6*, 88–95. [[CrossRef](#)]
6. Yin, Z.; Zhang, W.; Feng, F.; Zhang, Y.; Kang, W. α -Glucosidase inhibitors isolated from medicinal plants. *Food Sci. Hum. Wellness* **2014**, *3*, 136–174. [[CrossRef](#)]
7. Chen, J.; Zhang, X.; Huo, D.; Cao, C.; Li, Y.; Liang, Y.; Li, B.; Li, L. Preliminary characterization, antioxidant and α -glucosidase inhibitory activities of polysaccharides from *Mallotus furetianus*. *Carbohydr. Polym.* **2019**, *215*, 307–315. [[CrossRef](#)] [[PubMed](#)]
8. Lin, M.Z.; Chai, W.M.; Zheng, Y.L.; Huang, Q.; Ou-Yang, C. Inhibitory kinetics and mechanism of rifampicin on α -glucosidase: Insights from spectroscopic and molecular docking analyses. *Int. J. Biol. Macromol.* **2019**, *122*, 1244–1252. [[CrossRef](#)] [[PubMed](#)]
9. Wei, M.; Chai, W.M.; Yang, Q.; Wang, R.; Peng, Y. Novel Insights into the Inhibitory Effect and Mechanism of Proanthocyanidins from *Pyracantha fortuneana* Fruit on α -Glucosidase. *J. Food Sci.* **2017**, *82*, 2260–2268. [[CrossRef](#)]
10. Sun, Y.; Liu, J.; Li, L.; Gong, C.; Wang, S.; Yang, F.; Hua, H.; Lin, H. New butenolide derivatives from the marine sponge-derived fungus *Aspergillus terreus*. *Bioorgan. Med. Chem. Lett.* **2018**, *28*, 315–318. [[CrossRef](#)]
11. Liu, H.; Chen, Z.; Zhu, G.; Wang, L.; Du, Y.; Wang, Y.; Zhu, W. Phenolic polyketides from the marine alga-derived *Streptomyces* sp. OUCMDZ-3434. *Tetrahedron* **2017**, *73*, 5451–5455. [[CrossRef](#)]
12. Rizvi, T.S.; Hussain, I.; Ali, L.; Mabood, F.; Khan, A.L.; Shujah, S.; Rehman, N.U.; Al-Harrasi, A.; Hussain, J.; Khan, A.; et al. New gorgonane sesquiterpenoid from *Teucrium mascatense* Boiss, as α -glucosidase inhibitor. *S. Afr. J. Bot.* **2019**, *124*, 218–222. [[CrossRef](#)]
13. Wang, C.; Guo, L.; Hao, J.; Wang, L.; Zhu, W. α -Glucosidase Inhibitors from the Marine-Derived Fungus *Aspergillus flavipes* HN4-13. *J. Nat. Prod.* **2016**, *79*, 2977–2981. [[CrossRef](#)] [[PubMed](#)]
14. Lee, J.; Lee, J.; Kim, G.J.; Yang, I.; Wang, W.; Nam, J.W.; Choi, H.; Nam, S.J.; Kang, H. Mycosufurans A and B, Antibacterial Usnic Acid Congeners from the Fungus *Mycosphaerella* sp., Isolated from a Marine Sediment. *Mar. Drugs* **2019**, *17*, 422. [[CrossRef](#)] [[PubMed](#)]
15. Otálvaro, F.; Nanclares, J.; Vásquez, L.E.; Quiñones, W.; Echeverri, F.; Arango, R.; Schneider, B. Phenalenone-Type compounds from *Musa acuminata* var. “Yangambi km 5” (AAA) and Their Activity against *Mycosphaerella fijiensis*. *J. Nat. Prod.* **2007**, *70*, 887–890. [[CrossRef](#)] [[PubMed](#)]
16. Assante, A.; Camarda, L.; Merlini, L.; Nasini, G. Secondary metabolites from *Mycosphaerella ligulicola*. *Phytochemistry* **1981**, *20*, 1955–1957. [[CrossRef](#)]
17. Huang, H.; Feng, X.; Xiao, Z.; Liu, L.; Li, H.; Ma, L.; Lu, Y.; Ju, J.; She, Z.; Lin, Y. Azaphilones and *p*-Terphenyls from the Mangrove Endophytic Fungus *Penicillium chermesinum* (ZH4-E2) Isolated from the South China Sea. *J. Nat. Prod.* **2011**, *74*, 997–1002. [[CrossRef](#)]
18. Liu, Y.; Yang, Q.; Xia, G.; Huang, H.; Li, H.; Ma, L.; Lu, Y.; He, L.; Xia, X.; She, Z. Polyketides with α -Glucosidase Inhibitory Activity from a Mangrove Endophytic Fungus, *Penicillium* sp. HN29-3B1. *J. Nat. Prod.* **2015**, *78*, 1816–1822. [[CrossRef](#)]
19. Liu, Z.; Chen, S.; Qiu, P.; Tan, C.; Long, Y.; Lu, Y.; She, Z. (+)- and (–)-Ascomlactone A: A pair of novel dimeric polyketides from a mangrove endophytic fungus *Ascomycota* sp. SK2YWS-L. *Org. Biomol. Chem.* **2017**, *15*, 10276–10280. [[CrossRef](#)] [[PubMed](#)]
20. Cui, H.; Liu, Y.; Nie, Y.; Liu, Z.; Chen, S.; Zhang, Z.; Lu, Y.; He, L.; Huang, X.; She, Z. Polyketides from the Mangrove-Derived Endophytic Fungus *Nectria* sp. HN001 and Their α -Glucosidase Inhibitory Activity. *Mar. Drugs* **2016**, *14*, 86. [[CrossRef](#)] [[PubMed](#)]
21. Liu, Y.; Xia, G.; Li, H.; Ma, L.; Ding, B.; Lu, Y.; He, L.; Xia, X.; She, Z. Vermistatin Derivatives with α -Glucosidase Inhibitory Activity from the Mangrove Endophytic Fungus *Penicillium* sp. HN29-3B1. *Planta Med.* **2014**, *80*, 912–917. [[CrossRef](#)] [[PubMed](#)]
22. Kemami Wangun, H.V.; Ishida, K.; Hertweck, C. Epicoccalone, a Coumarin-Type Chymotrypsin Inhibitor, and Isobenzofuran Congeners from an *Epicoccum* sp. Associated with a Tree Fungus. *Eur. J. Org. Chem.* **2008**, *22*, 3781–3784. [[CrossRef](#)]
23. Nam, H.L.; James, B.G.; Donald, T.W. Isolation of Chromanone and Isobenzofuran Derivatives from a Fungicolous Isolate of *Epicoccum purpurascens*. *Bull. Korean Chem. Soc.* **2007**, *28*, 877–879.

24. Ferdinand, M.T.; Timothee, J.N.K.; Birger, D.; Clovis, D.M.; Hartmut, L. Paeciloside A, a new antimicrobial and cytotoxic polyketide from *Paecilomyces* sp. Strain CAFT156. *Planta Med.* **2012**, *78*, 1020–1023.
25. Talontsi, F.M.; Dittrich, B.; Schüffler, A.; Sun, H.; Laatsch, H. Epicoccolides: Antimicrobial and Antifungal Polyketides from an Endophytic Fungus *Epicoccum* sp. Associated with *Theobroma cacao*. *Eur. J. Org. Chem.* **2013**, *15*, 3174–3180. [[CrossRef](#)]
26. Zhu, H.; Chen, C.; Xue, Y.; Tong, Q.; Li, X.; Chen, X.; Wang, J.; Yao, G.; Luo, Z.; Zhang, Y. Asperchalsine A, a Cytochalasan Dimer with an Unprecedented Decacyclic Ring System, from *Aspergillus flavipes*. *Angew. Chem. Int. Ed.* **2015**, *54*, 13374–13378. [[CrossRef](#)] [[PubMed](#)]
27. Zhou, G.X.; Wijeratne, E.M.K.; Bigelow, D.; Pierson, L.S.; Vanetten, H.D.; Gunatilaka, A.A.L. Aspochalasins I, J, and K: Three New Cytotoxic Cytochalasans of *Aspergillus flavipes* from the Rhizosphere of *Ericameria laricifolia* of the Sonoran Desert. *J. Nat. Prod.* **2004**, *67*, 328–332. [[CrossRef](#)]
28. Da Silva Araújo, F.D.; de Lima Fávaro, L.C.; Araújo, W.L.; de Oliveira, F.L.; Aparicio, R.; Marsaioli, A.J. Epicolactone—Natural Product Isolated from the Sugarcane Endophytic Fungus *Epicoccum nigrum*. *Eur. J. Org. Chem.* **2012**, *27*, 5225–5230. [[CrossRef](#)]
29. Cai, R.; Wu, Y.; Chen, S.; Cui, H.; Liu, Z.; Li, C.; She, Z. Peniisocoumarins A–J: Isocoumarins from *Penicillium commune* QQF-3, an Endophytic Fungus of the Mangrove Plant *Kandelia candel*. *J. Nat. Prod.* **2018**, *81*, 1376–1383. [[CrossRef](#)]
30. Tan, C.; Liu, Z.; Chen, S.; Huang, X.; Cui, H.; Long, Y.; Lu, Y.; She, Z. Antioxidative Polyketones from the Mangrove-Derived Fungus *Ascomycota* sp. SK2YWS-L. *Sci. Rep.* **2016**, *6*, 36609. [[CrossRef](#)] [[PubMed](#)]



© 2019 by the authors. Licensee MDPI, Basel, Switzerland. This article is an open access article distributed under the terms and conditions of the Creative Commons Attribution (CC BY) license (<http://creativecommons.org/licenses/by/4.0/>).